Experimental Characterization of Diffraction Patterns from Transmission Gratings with Variable Line Densities

Carlos Mateo Perez Carvajal (00332636) and Ariel Alejandro Quelal Gamboa (00325160)
Experimental Physics 1
Universidad San Francisco de Quito
(Dated: March 5, 2025)

This study analyzes the diffraction patterns produced by a green laser beam (λ=510 - 570 nm) incident on transmission gratings with different line densities: 100, 300, and 600 lines/mm. The intensity of the diffracted light was measured as a function of the diffraction angle using a photodiode and a stepper motor controlled via Arduino. Theoretical predictions for the angular and spatial positions of diffraction maxima were obtained using the exact grating equation and compared against experimental measurements. While the general features of the Fraunhofer diffraction model were confirmed, significant discrepancies were observed in fringe spacing, particularly for lower-density gratings. Relative errors ranged from 13.6% (600 lines/mm) to over 85% (100 lines/mm), attributed to mechanical misalignment, photodiode resolution, and broadened peak profiles. These findings highlight both the strengths and limitations of low-cost diffractometer setups for quantitative optical analysis.

Keywords: Diffraction grating, Fraunhoffer diffraction, multi-slit interference, intensity distribution, diffraction angle.

I. INTRODUCTION

Diffraction gratings play a central role in optical systems that require precise spectral resolution, including applications in spectroscopy, telecommunications, and metrology. These devices disperse incident light into discrete angular maxima whose positions depend on both the wavelength and the spacing between grating lines. Understanding how diffraction behavior varies with grating line density is essential for the design and calibration of such systems.

In the Fraunhofer diffraction regime, the interference pattern produced by a multi-slit grating can be predicted using the grating equation, which relates the diffraction angle to the order number, wavelength, and slit spacing. As line density increases, diffraction orders appear at larger angles, and the resulting peaks become narrower and more intense.

This study explores the diffraction patterns generated by a green laser beam incident on transmission gratings with 100, 300, and 600 lines/mm. The angular intensity distribution was recorded using a photodiode mounted on a stepper motor-controlled stage, allowing for high-resolution scanning. Experimental measurements were compared to theoretical predictions obtained from the exact grating equation by translating diffraction angles into linear displacements on the detection plane.

While the qualitative features of the diffraction patterns agreed with theory, quantitative discrepancies (particularly in lower-density gratings) were observed. These were attributed to experimental limitations such as finite angular resolution, sensor alignment errors, and broadened peak shapes. The results underscore both the predictive value of the Fraunhofer model and the sensitivity of diffraction measurements to setup precision.

II. EXPERIMENTAL DETAILS

A. Experimental Procedure

The experimental setup, shown in Figure 1, was designed to measure the intensity distribution of the diffraction pattern produced by a green laser beam ($\lambda = 510 - 570$ nm) incident on a diffraction grating.A stepper motor was used to rotate a photodiode light sensor across different angular positions, ranging from $-40°$ to $40°$, measured from the axis determined by the laser beam. This configuration allowed a direct measurement of the diffracted light intensity as a function of angular position.

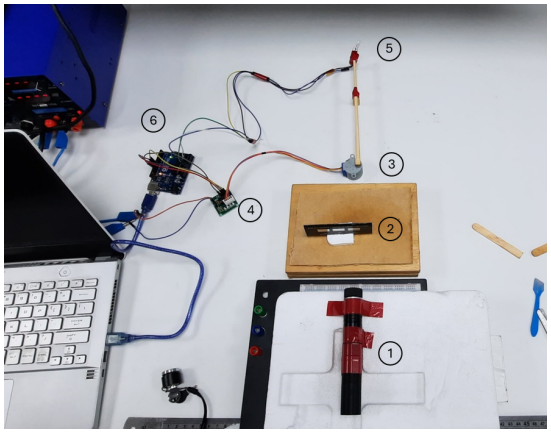

FIG. 1. The photograph of the diffractometer used to measure intensity distributions. ① Laser; ② Diffraction grating; ③ Stepper Motor 28 BYJ-48; ④ Module UNL2003; ⑤ Photodiode; ⑥ Arduino UNO

Initially, the green laser beam was directed through the diffraction grating, with the resulting diffraction pattern depending on the line density of the grating selected.

The stepper motor was set to an initial angle of approximately $-40°$, enabling the photodiode to begin measurements from this position and systematically move toward $40°$, capturing the variation in light intensity across the angular range.

The angular position of the light sensor was controlled employing an UNL2003 driver module, operated through Arduino code that specified the step size for each measurement cycle. The motor was configured to perform 3600 steps per full revolution, corresponding to an angular resolution of approximately $\sim 0.1°$ per step. The photodiode voltage signals were acquired using the Arduino's analog-to-digital converter, providing a voltage resolution of approximately ~ 4.9 mV.

B. Mathematical Model

To model the spacing of constructive interference peaks produced by diffraction gratings, we start with the classical grating equation and translate diffraction angles into linear coordinates at the detector plane.

A plane wave with wavelength $\lambda = 532$ [nm], incident normally on a transmission grating with groove spacing d, yields constructive interference maxima at angles θ_m satisfying

$$d \sin\theta_m = m\,\lambda$$

$$\theta_m = \arcsin\left(\frac{m\,\lambda}{d}\right) \tag{1}$$

where $m = 0, \pm1, \pm2, \ldots$ represents the diffraction order. For gratings with line densities N_ℓ of 600, 300, or 100 lines/mm, the groove spacing is

$$d = \frac{1}{N_\ell} \quad [\text{mm}], \qquad N_\ell = 600,\ 300,\ 100.$$

A detector located a distance $L = 20$ [cm] from the grating records each diffraction maximum at lateral displacement x_m from the central maximum (zero-order):

$$x_m = L\,\tan\theta_m = L\,\tan\Big(\arcsin\big(\tfrac{m\,\lambda}{d}\big)\Big) \tag{2}$$

Due to the large angles encountered for higher orders ($\theta_m \ll 1$ does not hold), no small-angle approximation is valid, requiring the exact formula to compute spacing between consecutive orders:

$$\Delta x_m = L\left[\tan\big(\arcsin\big(\tfrac{(m+1)\,\lambda}{d}\big)\big) - \tan\big(\arcsin\big(\tfrac{m\,\lambda}{d}\big)\big)\right] \tag{3}$$

Defining $\bar{\Delta}x_{\text{exp}}$ as the experimentally measured mean spacing, the percentage error between theoretical and experimental values is

$$\varepsilon_{\%} = 100\%\ \frac{\left|\bar{\Delta}x_{\text{exp}} - \Delta x_m\right|}{\Delta x_m}$$

III. RESULTS AND DISCUSSION

For the 600 lines/mm grating, the theoretical fringe spacing for the first diffraction order ($m = \pm1$) is $\Delta x_{\text{theo}} = 67.4$ [mm] (Eq. 3), while the experimental mean spacing is $\bar{\Delta}x_{\text{exp}} = 58.25$ [mm]. This corresponds to an absolute discrepancy of 9.15 [mm] and a relative error of 13.6%.

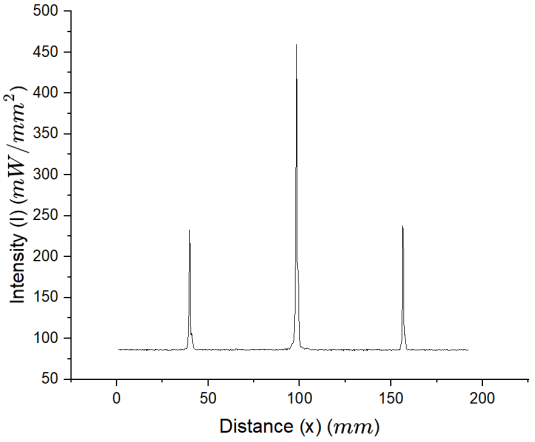

FIG. 2. Intensity profile for the 600 lines/mm grating.

Only the zero-order and first-order peaks were resolved in this dataset.

For the 300 lines/mm grating, the central maximum ($m = 0$) is located at 108.8 [mm]. The first-order peaks at 81.2 [mm] and 135.8 [mm] yield

$$\Delta x_{\text{exp},\,m=\pm1} = 27.3 \text{ [mm]},$$

whereas the theoretical prediction remains $\Delta x_{\text{theo},\,m=\pm1} = 67.4$ [mm]. The absolute discrepancy is 40.1 [mm], corresponding to a 59.5% error.

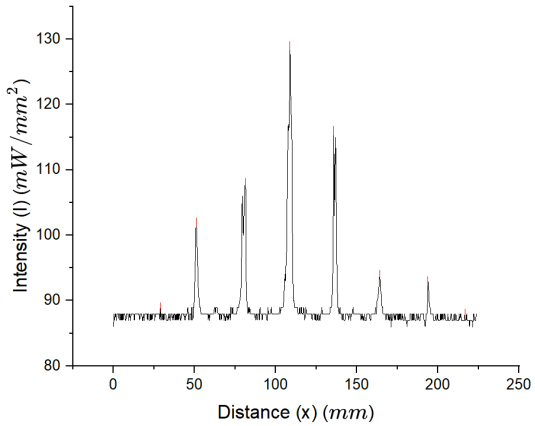

FIG. 3. Intensity profile for the 300 lines/mm grating.

Second-order peaks ($m = \pm2$) at 51.1 [mm] and 164.1 [mm] give

$$\Delta x_{\text{exp},\,m=\pm2} = 56.5 \text{ [mm]}, \quad \Delta x_{\text{theo},\,m=\pm2} = 139 \text{ [mm]},$$

with an absolute discrepancy of 82.5 [mm] (59.4% error).

Although higher-order peaks may be observed in this dataset, they are not suitable for comparison with the other gratings.

For the 100 lines/mm grating, the central maximum appears at 92.0 [mm]. The first-order peaks at 82.2 [mm] and 100.8 [mm] yield

$$\Delta x_{\text{exp},\, m=\pm1} = 9.3 \text{ [mm]}, \quad \Delta x_{\text{theo},\, m=\pm1} = 67.4 \text{ [mm]},$$

an absolute discrepancy of 58.1 [mm] (86.2% error).

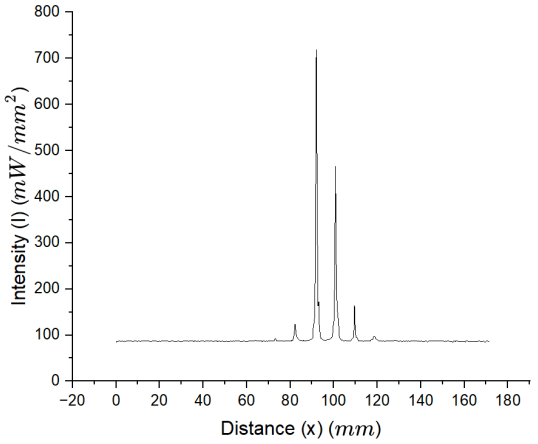

FIG. 4. Intensity profile for the 100 lines/mm grating.

Finally, second-order peaks at 73.5 [mm] and 109.9 [mm] give

$$\Delta x_{\text{exp},\, m=\pm2} = 18.2 \text{ [mm]}, \quad \Delta x_{\text{theo},\, m=\pm2} = 139 \text{ [mm]},$$

with an absolute discrepancy of 120.8 [mm] (86.9% error).

IV. CONCLUSION

This study quantified the discrepancies between theoretical and experimental fringe spacings for transmission gratings of 600, 300 and 100 lines/mm. By applying the exact grating equation and mapping diffraction angles to linear displacements at a fixed detector distance, we obtained predictions for multiple orders and compared them to measurements.

For the 600 lines/mm grating, the first-order spacing ($\Delta x_{\text{theo}} = 67.4$ [mm]) differed from the experimental mean ($\bar{\Delta} x_{\text{exp}} = 58.25$ [mm]) by an absolute 9.15 [mm] (13.6% relative error). This moderate discrepancy stems primarily from alignment uncertainties of the photodiode, finite sensor resolution, and small variations in groove spacing.

Lower-density gratings exhibited substantially larger relative errors: 59.5% for the 300 lines/mm first order and 86.2% for the 100 lines/mm first order. These increased errors reflect broader, less defined peaks due to wider groove spacing, heightened sensitivity to angular misalignment, and limited angular resolution of the detector.

The use of the exact spacing formula validated our theoretical model; however, mechanical instabilities and the detector's sampling constraints introduced measurement noise and reduced reproducibility. These limitations manifest most clearly in the diminished peak definition and in the larger scatter of successive measurements.

Future improvements should include the implementation of a vibration-isolated optical bench to minimize mechanical drift, the adoption of higher-resolution, higher-speed photodetectors for more precise peak localization, the use of automated alignment and angular-calibration routines to reduce systematic error, and finer control over grating positioning to enhance repeatability.

Overall, the results demonstrate that simple transmission-grating setups can closely approximate theoretical diffraction patterns when experimental uncertainties are controlled. This work provides a roadmap for refining optical metrology in both teaching laboratories and precision research applications.

[1] B. Edlén, The dispersion of standard air, Journal of the Optical Society of America **43**, 339 (1953).
[2] B. Edlén, The refractive index of air, Metrologia **2**, 71 (1966).
[3] M. Ducros, Determination of the refractive index of air from interferometric measurements with a low-cost setup, European Journal of Physics **42**, 035402 (2021).
[4] P. Hariharan, *Basics of Interferometry*, 2nd ed. (Academic Press, Burlington, MA, 2007).